Theoretical study of small clusters of indium oxide: InO, In$_2$O, InO$_2$, In$_2$O$_2$

Saikat Mukhopadhyay [a], S. Gowtham [a], Ravindra Pandey [a,*], Aurora Costales [b]

[a] Department of Physics, Michigan Technological University, Houghton, MI 49931, USA
[b] Departamento de Química Fisica y Analítica, Facultad de Química, Universidad de Oviedo, 33006 Oviedo, Spain

A B S T R A C T

The structural, vibrational and electronic properties of small clusters of indium oxide (In$_m$O$_n$; $m, n = 1, 2$) in the neutral and the ionic state are studied using first-principles method based on density functional theory. The linear structures are preferred over all the other possible structures for the neutral InO clusters. The structural deformations and the instability in InO, In$_2$O, InO$_2$ and In$_2$O$_2$ are relatively higher when an electron is removed than the case when an electron is added to it. In$_2$O, with negative electron affinity, is predicted to be highly unstable. The calculated results suggest that the neutral InO clusters are likely to become unstable when the metal to oxygen ratio is larger than unity.

© 2010 Elsevier B.V. All rights reserved.

1. Introduction

Indium oxide (In$_2$O$_3$) is the n type semiconductor with the band gap of 3.7 eV [1]. It is generally used as a resistive element in integrated circuits and in heterojunctions with p-InP, n-GaAs and other semiconductors. Tin doped indium oxide (ITO) is being used in devices like liquid crystal display (LCD) plasma, electromagnetic and organic light-emitting diode (OLED) displays. Recently, chromium doped In$_2$O$_3$ (e.g. In$_{2-x}$Cr$_x$O$_3$) has been reported as a magnetic semiconductor showing high temperature applications such as a spin injector material in spintronics [2]. In spite of applications in the bulk and thin film form of indium oxide, no systematic effort has been initiated to study the properties of indium oxide at nanoscale. We note that doped indium oxide has been a focus of recent theoretical [3] and experimental studies [4–7]. A theoretical study [8] based on discrete variational X$_\alpha$ method on the bulk fragments of In$_2$O$_3$ ascertained that the In–O bond is predominant in In$_2$O$_3$.

Small clusters of indium oxide can be considered as a prototype model to understand the physics and chemistry of structures at nanoscale. In addition to that, clusters do show distinct properties of their own apart from bridging molecular and bulk-like properties. In this work, we investigate the structural, vibrational and electronic properties of small clusters of indium oxide. The calculated results are then compared with the previously reported results on the aluminium [9] and gallium oxides [10] to see how the trend in structural and electronic properties matches or differs with cations in the group IIIA oxides.

2. Methodology

We have performed first-principles calculations solving the Kohn–Sham equations based on the density functional theory (DFT) on neutral and charged indium oxide clusters using the Gaussian 03 code [11]. The gradient-corrected B3LYP functional form (i.e. Becke's 3-parameter hybrid exchange functional [12] and Lee, Yang, and Parr correlation functional [13]) was employed for our calculations. We used Los Alamos National Laboratory (LANL2DZ [14]) basis sets for both indium and oxygen atoms in all our calculations.

All the clusters analyzed in this study have been fully optimized and the convergence criterion was 10^{-9} hartree for the energy and 10^{-4} hartree/Å for its gradient. The vibrational frequencies under the harmonic approximation, with analytical force constants were calculated and the positivity of the vibrational frequency confirms the stability of the corresponding lowest energy configuration leading to a true minima.

The selection of B3LYP functional form and LANL2DZ basis set was justified by performing calculations on the oxygen molecule for which the experimental values are available. Employing the LANL2DZ basis set the computed binding energy of O$_2$ with the PBE (PW91) functional forms [15,16], was found to be 5.14 (5.12) eV. It is in agreement with the experimental value of 5.16 eV [17] though the vibrational frequency of 1365 (1367) cm^{-1} was significantly underestimated compared to the experimental value of 1580 cm^{-1} [17]. B3LYP, on the other hand, underestimates the binding energy (4.11 eV) but yields the vibrational frequency of 1447 cm^{-1} in a much better way compared to that of PBE (PW91). The bondlength of O$_2$ was found to lie in the range 1.21–1.29 Å as compared to the experimental value (1.21 Å). We are aware of the

* Corresponding author. Tel.: +1 9064872086; fax: +1 9064872933.
  E-mail address: pandey@mtu.edu (R. Pandey).

fact that the use of LANL2DZ for indium may be acceptable [18,19] but not for oxygen. We have also performed calculations on the InO cluster with the 6-31G(∗) basis set for oxygen and LANL2DZ for indium. The calculated results did not change significantly from those obtained using LANL2DZ for both oxygen and indium.

3. Results and discussion

3.1. InO

The electronic states along with the structural properties of InO are shown in Table 1. For neutral InO, the ground state is $^2\Sigma$ as can be predicted from its electronic configuration. For the cationic and anionic InO, calculations find the most stable electronic state to be $^3\Sigma$ and $^1\Sigma$, respectively. The dissociation energies are calculated with respect to the atoms in their ground states. For InO$^-$ and InO$^+$ dissociation products, the electron added or removed was assigned to oxygen and indium atoms, respectively, in accordance with the respective Pauling's electronegativity values of 3.44 and 1.78.

The anionic InO is more stable than the neutral and cationic InO. The addition of an electron to the neutral InO, therefore, increases the strength of In–O bond. In the case of GaO, a similar feature was found [10]. The dissociation energy of 5.22 eV for the anionic GaO was found to be 0.93 eV higher than what is calculated for the cationic case. This fact can be explained in terms of the molecular orbital theory. When an extra electron is added to the neutral InO, that electron fills the semi-occupied molecular orbital (SOMO)

which has a σ-bonding character. In this way, the anionic cluster completes the molecular orbital leading to more stability. For the cationic molecule, the reverse takes place. The electron comes out from the σ-bonding highest occupied molecular orbital (HOMO) of the neutral molecule, reducing the stability of the cluster with a larger bond length and smaller frequency.

3.2. In$_2$O and InO$_2$

A schematic representation of all the initial geometries of triatomic clusters of indium oxide are shown in Fig. 1 and their geometric and energetic properties are collected in Table 2. To calculate the dissociation energies, we looked into the most favorable fragmentation reaction, shown in Table 2, among all other possible ones and defined the dissociation energy as the difference in energies of the products and the reactants.

In$_2$O: The neutral In$_2$O is found to be stable in $^1\Sigma$ state. Among all the possible initial geometries (see Fig. 1) of In$_2$O, the linear In–O–In ($D_{\infty h}$) is found to be the most stable with bond length (R_{In-O}) of 1.93 Å. The initial bent structure, namely ∠In–O–In was converged to In–O–In and the one with symmetry C_s converged to $C_{\infty v}$ symmetry during the process of optimization. The bond length R_{In-O} is now shortened compared to that of the InO.

The energy of the asymmetric linear structure (In–In–O) is about 3.2 eV higher than that of In–O–In. The metal–oxygen bonds are, therefore, preferred over the metal–metal bond in the neutral In$_2$O. It is consistent with the calculated bond energies 1.03 and 4.11 eV for In$_2$ and InO, respectively. The bond energies are calculated at B3LYP/LANL2DZ level of theory and defined as E(atoms) – E(cluster). The cationic and the anionic In$_2$O have been found to be in doublet electronic states. Even though the relative stability of the metal–oxygen bond over the metal–metal bond reduces in the ionized clusters compared to the neutral cluster, the preference of metal–oxygen bond over the metal–metal bond seems to govern the cationic as well as the anionic clusters of In$_2$O. The relative stability of cationic and anionic clusters is 1.63 and 1.44 eV, respectively. The most stable configuration is the linear In–O–In for both cases. R_{In-O} of the neutral In$_2$O does not change in the anionic

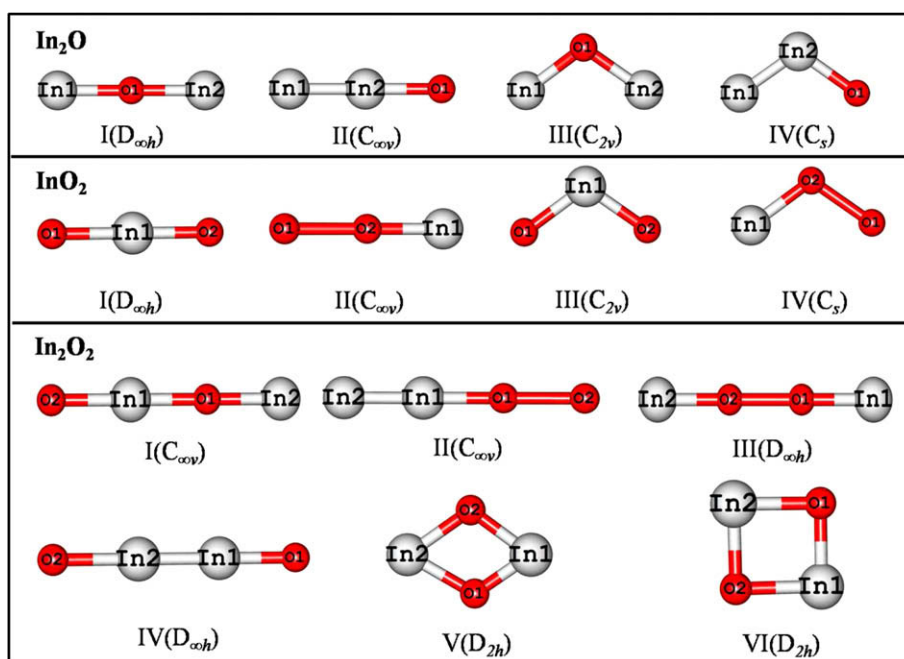**Table 1**
Electronic state, bond length (Å), dissociation energy (eV) and vibrational frequency (cm^{-1}) of neutral and ionized InO.

	$^{2S+1}\Lambda$	R_e (Å)	D_e (eV)[a]	ω_e (cm^{-1})
InO	$^2\Sigma$	2.06	3.48	469
InO$^+$	$^3\Sigma$	2.95	0.22	131
InO$^-$	$^1\Sigma$	1.89	4.90	625

[a] D_e = E(In) + E (O) − E (cluster).

Fig. 1. Schematic representation of the initial configurations of In$_2$O, InO$_2$ and In$_2$O$_2$. The larger and smaller circles represent the indium and oxygen atoms, respectively.

Table 2
Isomeric configurations of In_2O and InO_2 (see Fig. 1). ΔE is energy (eV) relative to the most stable configuration, stX represents the case where the optimization leads to the configuration X, R_{In-O} is the bond length (Å) and $\overline{D}_e$ is the dissociation energy (eV).

Isomer	I ($D_{\infty h}$)	II ($C_{\infty v}$)	III (C_{2v})	IV (C_s)	Most favorable fragmentation path	Fragmentation energy (eV)
In_2O						
ΔE	0.00	3.24	stI	stII	$In_2O \rightarrow InO + In$	4.95
R_{In-O}	1.93	1.82				
R_{In-In}		3.08				
$\overline{D}_e$	4.95	1.71				
In_2O^+						
ΔE	0.00	1.63	st1	stII	$In_2O^+ \rightarrow InO + In^+$	2.07
R_{In-O}	2.24	2.00				
R_{In-In}		3.51				
$\overline{D}_e$	2.07	0.43				
In_2O^-						
ΔE	0.00	1.44	0.08	2.48	$In_2O^- \rightarrow InO^- + In$	2.77
R_{In-O}	1.96	1.85	1.98	1.90		
R_{In-In}		3.09		3.29		
$\overline{D}_e$	2.77	1.33	2.69	0.30		
InO_2						
ΔE	0.19	0.00	2.77	stII	$InO_2 \rightarrow InO + O$	2.66
R_{In-O}	1.85	1.98	2.29			
R_{O-O}		1.37				
$\overline{D}_e$	2.48	2.66	0.11			
InO_2^+						
ΔE	3.10	0.00	stI	stII	$InO_2^+ \rightarrow InO^+ + O$	4.08
R_{In-O}	1.90	2.82				
R_{O-O}		1.26				
$\overline{D}_e$	0.98	4.08				
InO_2^-						
ΔE	0.00	1.96	stI	stII	$InO_2^- \rightarrow InO^- + O$	3.75
R_{In-O}	1.85	1.91				
R_{O-O}		1.43				
$\overline{D}_e$	3.75	1.80				

case but increases to 2.24 Å for the cationic In_2O, suggesting that the deformation is larger when the electron is removed as compared to the case when the electron is added to the neutral In_2O.

In neutral and ionized In_2O, the degenerate modes (see Table 3) represent out of plane bending movements and the last two modes correspond to the symmetric and asymmetric stretching of In–O bonds.

InO₂: The neutral structures of InO_2 are found to have doublet electronic state. The linear structure with the symmetry $C_{\infty v}$ is found to be the most stable. The initial bent structure (∠O–O–In) converges to the linear one (O–O–In) during the process of optimization. The stability of InO_2 is predominantly determined by the

Table 3
Frequency values (ω) in cm⁻¹ of the normal modes of vibration for the neutral, anionic, and cationic clusters.

Cluster	Symmetry	Frequency (mode)
In_2O		
$q = 0$	$D_{\infty h}$	112 (π_u), 203 (σ_g), 765 (σ_u)
$q = -1$	$D_{\infty h}$	132 (π_u), 190 (σ_g), 559 (σ_u)
$q = +1$	$D_{\infty h}$	62 (π_u), 126 (σ_g), 414 (σ_u)
InO_2		
$q = 0$	$C_{\infty v}$	83 (π), 353 (σ), 1146 (σ)
$q = -1$	$D_{\infty h}$	138 (π_u), 634 (σ_g), 709 (σ_u)
$q = +1$	$C_{\infty v}$	39 (π), 84 (σ), 1457 (σ)
In_2O_2		
$q = 0$	$C_{\infty v}$	68 (π), 168 (π), 206 (σ) 709 (σ), 821 (σ)
$q = -1$	D_{2h}	101 (b_{3u}), 189 (a_g), 217 (b_{2u}), 386 (b_{2u}), 489 (a_g), 516 (b_{1u})
$q = +1$	$C_{\infty v}$	63 (π), 179 (π), 184 (σ_g) 534 (σ), 773 (σ)

bond between the similar atoms (O–O) rather than the metal–oxygen bond as the former one is energetically more favorable. The R_{O-O} is 7.9% larger than that of a oxygen molecule whereas the R_{In-O} is 4% smaller than that of InO.

Among the normal modes of vibration, the degenerate modes, 83 (π), correspond to the out of plane bending and the rest represent the symmetric and asymmetric stretching of O–In and O–O bonds, respectively. The O–O bond length (1.40 Å) was found to be higher than that of the oxygen molecule (1.21 Å) and the stretching frequency of O–O bond (1146 cm⁻¹) was found to be lower than that of the oxygen molecule (1659 cm⁻¹).

The triplet and singlet electronic states are found to be the most stable for the cationic and anionic clusters of InO_2, respectively. Among all the initial structures of the cationic InO_2, the linear one with $C_{\infty v}$ symmetry (O–O–In) is the most stable one. The R_{O-O} of 1.26 Å is very close to that of an oxygen molecule, 1.21 Å. R_{In-O} of 2.82 Å is much larger than that of InO. The ground state of cationic InO_2, therefore, appears to be an oxygen molecule weakly attached to In. This can also be verified from the normal modes of vibration. The highest frequency (1457 cm⁻¹) is close to that of the vibrational frequency of an oxygen molecule (1659 cm⁻¹). The degenerate modes of vibration represent the bending movements which are out of plane and the one with frequency 84 (σ) is for the soft stretching of the In–O bond.

The linear structure O–In–O with $D_{\infty h}$ symmetry leads to the most stable configuration for the anionic InO_2. The two In–O bonds are found to be equal to each other with the bond length of (1.85 Å). This is very close to the one what we found in the case of anionic InO. The anionic InO_2 can be considered as an oxygen atom attached to the anionic InO, which in a way supports the fragmentation path given in Table 2.

3.3. In_2O_2

All the initial geometries of In_2O_2 which we considered are shown in Fig. 1. The total energies of the neutral clusters are computed in the singlet and triplet electronic states and the calculated results found that the singlet electronic state results in the ground state configuration for neutral In_2O_2. The bond lengths and energy of the most stable configuration and a comparative study with the other configurations of the neutral as well as the ionic clusters can be found in Table 4. Among all the initial configurations the linear structure O–In–O–In is found to be the most stable one for neutral In_2O_2. The In–O bond length is found to be 1.87 Å (the average of the three In–O bond is taken) which is smaller than In–O.

The relative stability of all the structures considered for In_2O_2 can be interpreted considering the bond energies which are calculated as 1.03, 3.48 and 4.11 eV for In–In, In–O and O–O bonds, respectively.

Accordingly, it can be said that III-$D_{\infty h}$ should have the lowest energy among the linear ones. But III-$D_{\infty v}$ is 1.79 eV higher in energy than I-$C_{\infty v}$. This is due to the charge transfer from In to O atom resulting in an elongation in the O–O bond length. Note that the linear configurations – I, II, III and IV in Fig. 1 – are found to be singlet with Π symmetry. More interestingly, in the case of V-D_{2h} and VI-D_{2h}, it is realized that even though they are expected to be more stable than the linear structures from the bond energetics point of view, they are 0.87 and 0.46 eV higher in energy relative to the ground state, I-$C_{\infty v}$. The electrostatic repulsion between cluster atoms yields a larger R_{In-O} in the low lying clusters of In_2O_2.

It is easy to recognize the stretching frequency of InO in the frequency spectrum of In_2O, InO_2 and In_2O_2, which gets modified depending on the coordination index in the given cluster (see Table 3).

From the Mulliken analysis (see Table 5), we find that the atomic charges are distributed uniformly, with opposite signs for InO, but that is not the case for In_2O_2. For the most stable neutral and cationic structures of In_2O_2, it is noticed that the inner atoms [i.e. In(1) and O(1), see Fig. 1] are more ionic relative to the outer ones [i.e. In(2) and O(1), see Fig. 1]. The non-uniformity in the charge distribution can also be seen in the charge density plots (not shown here), and is likely to be due to the different coordination numbers for atoms in the linear configuration of In_2O_2.

Table 5
Mulliken charges ($\|e\|$) for oxygen and indium atoms in the most stable neutral and ionized clusters of InO, In_2O, InO_2 and In_2O_2.

	InO			In$_2$O and InO$_2$	
	Q_{In}	Q_O		Q_{In}	Q_O
InO	0.53	−0.53	In_2O	0.50	−1.01
InO^-	−0.12	−0.88	In_2O^-	−0.02	−0.95
InO^+	0.91	0.09	In_2O^+	0.78	−0.57
			InO_2	0.62	(−0.500 −0.12)
			InO_2^-	0.74	−0.87
			InO_2^+	0.95	(−0.08 0.13)
			In_2O_2		
	Q_{In_1}	Q_{In_2}	Q_{O_1}	Q_{O_2}	
In_2O_2	1.13	0.62	−1.04	−0.74	
$In_2O_2^-$	0.33		−0.83		
$In_2O_2^+$	1.49	0.82	−0.35	−0.96	

All the ionized clusters of In_2O_2 have doublet electronic state. The neutral cluster configuration does not undergo significant changes in its cationic state. On the other hand, the distorted rhombus shaped structure [Fig. 1 – Isomer V (D_{2h})] is found to be the most stable in the anionic state. Here R_{In-In} is 3.43 Å suggesting a less electrostatic repulsion between the In atoms in the anionic cluster.

The most favorable fragmentation reactions for the most stable structures of neutral and the ionized In_2O_2 are shown in Table 4. The fragmentation energy of the neutral, cationic and anionic In_2O_2 is 2.50, 0.93 and 1.09 eV, respectively. The lower fragmentation energy for the ionic In_2O_2 suggests that the fragmentation is more likely to take place for the ionized clusters of In_2O_2 compared to that of the neutral one. Additionally, we have considered the fragmentation of the neutral In_2O_2 with respect to In_2 and O_2. The calculated energy comes out to be about 25.6 eV suggesting a very high stability of In_2O_2.

3.4. Electronic properties of InO, In_2O, InO_2 and In_2O_2

The vertical and adiabatic electron affinity (EA) and ionization potential (IP) are calculated (see Table 6) for InO, In_2O, InO_2 and In_2O_2 in their most stable configurations. The definition of EA and IP we employed is as follows:

Table 4
Isomeric configurations of In_2O_2. ΔE is energy (eV) relative to the most stable structure, R_{In-O} is the bond length (Å) and $\overline{BE}$ is the binding energy per atom (eV).

Isomer	I ($C_{\infty v}$)	II ($C_{\infty v}$)	III ($D_{\infty h}$)	IV ($D_{\infty h}$)	V (D_{2h})	VI (D_{2h})	Most favorable fragmentation path
In_2O_2							
ΔE	0.00	4.82	1.80	2.75	0.87	0.46	$In_2O_2 \rightarrow In_2O + O$
R_{In-O}	1.87[a]	1.85	1.92	1.82	2.17	1.99	
R_{In-In}		3.05		2.79	4.01	2.92	
R_{O-O}		1.38	1.43		1.63	2.73	
$\overline{BE}$	4.12	2.92	3.67	3.43	3.90	4.01	
$In_2O_2^-$							
ΔE	2.34	2.15	3.07	2.15	0.00	0.60	$In_2O_2^- \rightarrow InO_2^- + In$
R_{In-O}	2.12[a]	1.86	1.89	1.86	2.07	2.12	
R_{In-In}		3.09		3.47	3.43	3.33	
R_{O-O}		1.42	2.09		2.33	2.61	
$\overline{BE}$	3.92	3.96	3.73	3.96	4.50	4.35	
$In_2O_2^+$							
ΔE	0.00	4.57	0.76	3.81	1.47	0.68	$In_2O_2^+ \rightarrow InO_2 + In^+$
R_{In-O}	1.93[a]	2.00	2.17	2.02[a]	2.15	1.99	
R_{In-In}		3.52		3.48	3.77	2.88	
R_{O-O}		2.57	1.35		2.05	2.74	
$\overline{BE}$	2.09	0.94	1.90	1.14	1.72	1.92	

[a] The average bond length is taken; for $q = 0$: $R_{In_2-O_1} = 1.93$ Å, $R_{O_1-In_1} = 1.86$ Å, $R_{In_1-O_2} = 1.81$ Å; for $q = +1$: $R_{In_2-O_1} = 2.01$ Å, $R_{O_1-In_1} = 1.82$ Å, $R_{In_1-O_2} = 1.95$ Å; please refer to Fig. 1 for labeling of atoms.

Table 6
Vertical and adiabatic values (eV) of the electron affinity and ionization potential for InO, InO_2, In_2O and In_2O_2.

	InO	InO_2	In_2O	In_2O_2
Vertical EA	2.01	2.91	−0.46	3.48
Adiabatic EA	1.79	2.72	−0.08	1.63
Vertical IP	9.01	8.71	7.56	8.35
Adiabatic IP	9.01	7.62	8.71	8.16

Table 7
HOMO-LUMO gap in eV of InO, InO_2, In_2O and In_2O_2.

	Neutral	Anion	Cation
InO	4.49	2.37	0.30
InO_2	3.84	4.65	6.23
In_2O	4.38	3.84	5.17
In_2O_2	4.49	1.99	3.35

$$EA_{adiabatic} = E_{tot}(M, R_n) - E_{tot}(M^-, R_a) \qquad (1)$$

$$EA_{vertical} = E_{tot}(M, R_a) - E_{tot}(M^-, R_a) \qquad (2)$$

$$IP_{adiabatic} = E_{tot}(M^+, R_c) - E_{tot}(M, R_n) \qquad (3)$$

$$IP_{vertical} = E_{tot}(M^+, R_n) - E_{tot}(M, R_n) \qquad (4)$$

In Eqs. (1)–(4), M stands for the neutral, M^- for its anion and M^+ for its cation, whereas, R_n, R_a and R_c represents the equilibrium ground state geometry of the neutral, anion and cation, respectively.

The electron affinity of In_2O is found to be negative which implies that the anionic In_2O is less stable as compared to the neutral one. This is not surprising because Al_2O is reported to be too reactive to produce experimentally[9] and the electron affinity of Ga_2O, however, is predicted[10] to be very (∼0.03 eV). Therefore, we may conclude that the group III metal oxides are likely to become more unstable when the metal to oxygen ratio is larger than unity. Also, we have found that the adiabatic electron affinity increases when we add the oxygen to a cluster and the reverse happens when the metal atom is added. In this context, we find a strong similarity with the study on GaO [10] and AlO [9]. It is important to notice that the adiabatic and vertical ionization potential of InO are the same since there is no change in the nuclear coordinates during the addition of the electron to the neutral InO.

The HOMO–LUMO gaps are calculated (see Table 7) for the neutral and ionized clusters of InO, In_2O, InO_2 and In_2O_2. The HOMO–LUMO gap is considered as the energy difference between the HOMO and LUMO irrespective of the fact that orbitals are of α-type or the β-type. It is noticeable that the gap depends on the ratio of indium and oxygen present in the cluster. We expect fluctuations in the HOMO–LUMO gap as we increase the size of stoichiometric clusters before approaching the bulk value. It should be noted that the description of HOMO–LUMO gap may include the errors which inherently get introduced due to the usage of the hybrid functional [20].

4. Conclusions

The calculations using DFT-B3LYP/LANL2DZ level of theory find that the linear configurations are preferred over all other possible ones for all the neutral indium oxide clusters considered. The ionization induced distortions in the ground state of the respective neutral clusters are found relatively higher when an electron is removed compared to the case where an electron is added to it. The HOMO–LUMO gap is found to depend on the metal to oxygen ratio in the clusters. We find that both the vertical and adiabatic electron affinity of In_2O is negative which indicates that it is highly unstable in the ionic environment and therefore very difficult to produce experimentally. Our results predict that the group IIIA-metal oxides are likely to become unstable when the metal to oxygen ratio is larger than unity.

References

[1] Z.M. Jarzebski, Phys. Status Solid A 71 (1982) 13.
[2] J. Moodera, Nat. Mater. (2006), April issue.
[3] H. Odaka, Y. Shigesato, T. Murakami, S. Iwata, Jpn. J. Appl. Phys. 40 (2001) 3231.
[4] Fang Chen, Z. Huang, N. Tao, Appl. Phys. Lett. 91 (2007) 162106.
[5] C.J. Fan, B.J. Goodenough, J. Appl. Phys. 48 (1977) 3524.
[6] H. Zhang, X. Chen, Z. Li, L. Liu, T. Yu, Z. Zou, J. Phys. Condens. Mat. 19 (2007) 376213.
[7] F. Matino, L. Persano, V. Arima, V. Pisignano, R.I. Blyth, R. Cingolani, R. Rinaldi, Phys. Rev. B 72 (2005) 085437.
[8] I. Tanaka, M. Mizuno, H. Adachi, Phys. Rev. B 56 (1997) 3536.
[9] S.R. Desai, H. Wu, C.M. Rohlfing, L. Wang, J. Chem. Phys. 106 (1997) 1309.
[10] S. Gowtham, A. Costales, R. Pandey, J. Phys. Chem. B 108 (2004) 17295.
[11] Gaussian 03, M.J. Frisch, G.W. Trucks, H.B. Schlegel, G.E. Scuseria, M.A. Robb, J.R. Cheeseman, J.A. Montgomery Jr., T. Vreven, K.N. Kudin, J.C. Burant, J.M. Millam, S.S. Iyengar, J. Tomasi, V. Barone, B. Mennucci, M. Cossi, G. Scalmani, N. Rega, G.A. Petersson, H. Nakatsuji, M. Hada, M. Ehara, K. Toyota, R. Fukuda, J. Hasegawa, M. Ishida, T. Nakajima, Y. Honda, O. Kitao, H. Nakai, M. Klene, X. Li, J.E. Knox, H.P. Hratchian, J.B. Cross, V. Bakken, C. Adamo, J. Jaramillo, R. Gomperts, R.E. Stratmann, O. Yazyev, A.J. Austin, R. Cammi, C. Pomelli, J.W. Ochterski, P.Y. Ayala, K. Morokuma, G.A. Voth, P. Salvador, J.J. Dannenberg, V.G. Zakrzewski, S. Dapprich, A.D. Daniels, M.C. Strain, O. Farkas, D.K. Malick, A.D. Rabuck, K. Raghavachari, J.B. Foresman, J.V. Ortiz, Q. Cui, A.G. Baboul, S. Clifford, J. Cioslowski, B.B. Stefanov, G. Liu, A. Liashenko, P. Piskorz, I. Komaromi, R.L. Martin, D.J. Fox, T. Keith, M.A. Al-Laham, C.Y. Peng, A. Nanayakkara, M. Challacombe, P.M.W. Gill, B. Johnson, W. Chen, M.W. Wong, C. Gonzalez, J.A. Pople, Gaussian, Inc., Wallingford CT, 2004.
[12] A.D. Becke, J. Chem. Phys. 98 (1993) 5648.
[13] C. Lee, W. Yang, R.G. Parr, Phys. Rev. B 37 (1988) 785.
[14] J.P. Hay, R.W. Wadt, J. Chem. Phys. 82 (1985) 270.
[15] P.J. Perdew, K. Burke, M. Ernzerhof, Phys. Rev. Lett. 77 (1996) 3865.
[16] J.P. Perdew, in: P. Ziesche, H. Eschrig (Eds.), Electronic Structure of Solids 91, Akademie Verlag, Berlin, 1991, p. 11.
[17] P.K. Huber, G. Herzberg, Molecular Spectra and Molecular Structure. IV. Constants of Diatomic Molecules, Van Nostrand Reinhold Company, New York, 1979.
[18] D.A. Wann, S.L. Hinchley, H.E. Robertson, M.D. Francis, J.F. Nixon, D.W.H. Rankin, J. Organometal. Chem. 692 (2007) 1161.
[19] H. Tachikawa, H. Kawabata, Thin Solid Films 516 (2008) 3287.
[20] G. Zhang, B.C. Musgrave, J. Phys. Chem. A 111 (2007) 1554.